

What can the spatial distribution of galaxy clusters tell about their scaling relations?

Andrés Balaguera-Antolínez

Argelander Institute für Astronomie, Universität Bonn, Auf dem Hügel 71, D-53121 Bonn, Germany
e-mail: abalan@astro.uni-bonn.de

Received /Accepted

ABSTRACT

Context. The clustering of galaxy clusters is not only sensitive to the cosmological model and the parameters it is characterized by, but also to the links between cluster intrinsic properties –e.g., the X-ray luminosity, X-ray temperature– and the total cluster mass.

Aims. We aim to quantify the capability of the inhomogeneous distribution of galaxy clusters, represented by the two-point statistics in Fourier space, to retrieve information on the underlying scaling relations. As an example, we use the mass-X ray luminosity of galaxy clusters. We define the luminosity-weighted power spectrum and introduce the *luminosity power spectrum* as a direct assessment of the clustering of X-ray luminosity.

Methods. Using a suite of halo catalogs extracted from N -body simulations and realistic estimates of the mass-X ray luminosity relation, we measure the luminosity-weighted and the luminosity power spectrum of galaxy clusters. By means of a Fisher matrix analysis, we quantify the content of information (by means of a Figure-of Merit) encoded in the amplitude, shape and full-shape of these probes.

Results. The full shape of the luminosity power spectrum, when analyzed up to scales of $k \sim 0.2 h \text{Mpc}^{-1}$, yields a figure of merit which is only one order of magnitude below the value encoded in X-ray luminosity function estimated from the same sample. This is a significant improvement with respect to the FoM obtained from the estimates of the unweighted power spectrum.

Conclusions. The measurements of the clustering of galaxy clusters and its explicit dependence on the cluster observables (identified as cluster intrinsic properties) can contribute to improve the degree of knowledge regarding the underlying link between the property and the cluster masses. We therefore suggest future clustering analysis of galaxy clusters to take advantage of the luminosity power spectrum when aiming at simultaneously constraining cosmological and astrophysical parameters.

Key words. Cosmology: large-scale structure of the Universe – Galaxies: clusters: general – X-rays: galaxies: clusters

1. Introduction

The current understanding of the observed abundance and clustering of galaxy clusters relies on the large-scale statistical properties of dark matter haloes (e.g. Bardeen et al. 1986; Jenkins et al. 2001; Smith et al. 2003; Warren et al. 2006; Tinker et al. 2008). The mapping between cluster observables (e.g., X-ray luminosities, X-ray temperatures) and cluster mass is, accordingly, an ingredient of paramount relevance in the process of retrieving cosmological information from galaxy cluster experiments (see e.g. Pierpaoli et al. 2003; Stanek et al. 2006, 2010; Allen et al. 2011; Semboloni et al. 2012; Planck Collaboration et al. 2013). That mapping, referred to as the *cluster scaling relations*, represents a simple way to characterize the complex baryonic processes taking place within galaxy clusters (see e.g. Sarazin 1988; Mo et al. 2010; Stanek et al. 2010; Kravtsov & Borgani 2012).

The cluster scaling relations are often calibrated by direct measurements of cluster intrinsic properties and masses (e.g. Finoguenov et al. 2001; Stanek et al. 2006; Giodini et al. 2009; Pratt et al. 2009; Planck Collaboration et al. 2011). These measurements strongly depend on aspects such as the definition of mass and the dynamical state of galaxy clusters (e.g. Rasia et al. 2012), potentially plaguing their usefulness with systematic effects. In view of this, for cosmological applications, some studies adopt a self-calibrated approach in which the scaling rela-

tions are jointly constrained with the cosmological parameters (e.g. Mantz et al. 2010; Rapetti et al. 2013), using the cluster abundance as cosmological probe (e.g. Böhringer et al. 2002; Vikhlinin et al. 2009; Allen et al. 2011; Planck Collaboration et al. 2013).

Beyond the one-point statistics of galaxy clusters, their spatial distribution, often statistically characterized by the power spectrum $P(k)$ or its Fourier counterpart, the two-point correlation function $\xi(r)$ (e.g. Peebles 1980), can provide insights into the links between light and matter at the cluster scales (e.g. Pillepich et al. 2012). A simple example of this is the phenomenon of halo-bias, i.e., the increase of the halo clustering strength as a function of the halo mass (e.g. Kaiser 1986; Mo & White 1996; Sheth & Tormen 1999; Tinker et al. 2005; Pillepich et al. 2010; Porciani 2013). Observationally, such behavior has been detected as a function of intrinsic properties such as the X-ray luminosity (e.g. Schuecker et al. 2001; Balaguera-Antolínez et al. 2011), allowing us to explore the attributes of the scaling relation by means of the *amplitude* of the clustering signal. We refer to this as the *indirect* clustering-dependence upon intrinsic properties. On the other hand, a *direct* scrutiny of the impact of cluster intrinsic properties in the clustering pattern can be achieved by means of the so-called marked (or weighted) statistics (e.g. Schlather 2001). Marked statistics has been applied to galaxy redshift samples (e.g. Sheth 2005; Skibba et al. 2006;

Skibba & Sheth 2009; White & Padmanabhan 2009) as an attempt to explore the clustering of a given intrinsic property.

In this paper we quantify the capability of the three dimensional clustering signal of galaxy clusters to retrieve information of the underlying cluster scaling relations, represented here by the link between the cluster masses and X-ray luminosities. To this end, we measure the two-point marked-statistics in Fourier space by means of the luminosity-weighted power spectrum and the luminosity power spectrum. The latter is introduced –to our knowledge– for the first time in this paper, as an attempt to explicitly study the X-ray luminosity dependence of the clustering of galaxy clusters. We use a suite of halo catalogs built from N-body simulations together with a realistic estimate of cluster scaling relations, and carry out a Fisher-matrix analysis in order to determine the sensitivity of these probes to the parameters characterizing the scaling relation. We stress that our analysis is not a forecast for a particular experiment in view of a given cosmological model. Instead, we present a comparison between different clustering-related probes that can be implemented in forthcoming galaxy cluster samples in order to extract astrophysical and cosmological information. Our findings suggest that the direct assessment of the clustering of X-ray luminosity (or other physical properties) can help to establish tight constraints on the cluster scaling relations.

The outline of this paper is as follows. In Section 2 we introduce the suite of N-body simulations and the scaling relations used to assign observables to the dark matter haloes. We introduce the cluster luminosity-weighted power spectrum and the luminosity power spectrum and define a set of observables from which the information on the scaling relation will be retrieved. In Section 3 we evaluate the information content in those observables. We summarize our conclusions in Section 4.

2. Probes for cluster scaling relations

2.1. Halo catalogs and cluster scaling relation

We base our analysis on the L-BASICC N-body simulations (Angulo et al. 2008), represented by a suite of $N = 50$ realizations of the same flat Λ CDM cosmological model at redshift zero. The simulations are characterized by a matter density parameter $\Omega_{\text{mat}} = 0.237$, a baryon density parameter $\Omega_{\text{ba}} = 0.046$, a dimensionless Hubble parameter $h = 0.73^1$, a linear rms mass fluctuations within $8 h^{-1} \text{Mpc}$ of $\sigma_8 = 0.773$ and a scalar spectral index $n_s = 0.997$, following the evolution of 448^3 dark matter particles in a comoving box with volume $V = (1340 h^{-1} \text{Mpc})^3$. Halo catalogs were built by means of a friends-of-friends algorithm, characterized with a linking length of 0.2 times the mean inter-particle separation and a minimum mass of $1.73 \times 10^{13} h^{-1} M_{\odot}$ (ten dark matter particles).

We assign X-ray luminosities² L to dark matter haloes by means of a log-normal conditional probability distribution $\mathcal{P}(L|M)dL$ (hereafter scaling relation), specifying the probability of a cluster to have an X-ray luminosity in the range $L, L + dL$, conditional on its mass M :

$$\mathcal{P}(L|M)dL = \frac{1}{\sqrt{2\pi}\tilde{\sigma}} \exp\left[-\frac{1}{2\tilde{\sigma}^2}(\ell - \langle\ell|M\rangle)^2\right] d\ell, \quad (1)$$

where $\ell \equiv \log(L/(10^{44} \text{erg s}^{-1} h^{-2}))$ and $\tilde{\sigma}$ denotes the intrinsic scatter in ℓ at a fixed mass scale M , i.e., $\tilde{\sigma}^2 = \langle\ell^2|M\rangle - \langle\ell|M\rangle^2$.

¹ The Hubble constant H_0 in units of $100 \text{ km s}^{-1} \text{Mpc}^{-1}$.

² If not explicitly written, X-ray luminosities and masses are expressed in units of $10^{44} \text{erg s}^{-1} h^{-2}$ and $10^{14} h^{-1} M_{\odot}$ respectively.

For the mean of the scaling relation we use a power-law with amplitude α and slope γ ,

$$\langle\ell|M\rangle = \alpha + \gamma \log\left(\frac{M}{10^{14} h^{-1} M_{\odot}}\right). \quad (2)$$

As fiducial values we use $\alpha = -0.64$, $\gamma = 1.27$ and $\sigma = 0.15$, with $\sigma = \tilde{\sigma}/\ln(10)$. These numbers follow from realistic estimates of cluster mass-X ray luminosity relation (e.g. Balaguera-Antolínez et al. 2012). However, the exact figures are not relevant for the purposes of this work, as long as we are not constructing galaxy cluster catalogs constrained to follow a particular selection function. The Fisher matrix analysis presented in Sect. 3 will be dedicated to the sensitivity of a set of observables – to be defined in Sect. 2.2 – to the set of parameters $\{\mathcal{X}\} \equiv \{\alpha, \gamma, \sigma\}$.

For the forthcoming analysis, we consider objects with luminosities within the range $3 \times 10^{42} \leq L/(\text{erg s}^{-1} h^{-2}) \leq 5 \times 10^{44}$, which leads to realizations with $N_{\text{cl}} \sim 4 \times 10^5$ entries. In order to study the dependence of clustering with luminosity, we split this range in $n_{\ell} = 10$ disjoint and equally log-spaced bins. When the luminosity dependence is not explicitly shown in the forthcoming expressions, it is assumed that clusters with luminosities in the full luminosity range have been considered for the analysis.

2.2. Clustering estimates

Let $n_w(\mathbf{r}; L)$ denote the number density of weighted (or marked) haloes at a position \mathbf{r} and luminosity L , and $\bar{n}_w(L)$ its mean value. We aim to measure the luminosity-weighted power spectrum by defining the fluctuation $\delta_w(\mathbf{r}; L) \equiv (n_w(\mathbf{r}; L) - \bar{n}_w(L))/\bar{n}_w(L)$. Similarly, let $\delta_h(\mathbf{r}; L) \equiv (n(\mathbf{r}; L) - \bar{n}(L))/\bar{n}(L)$ denotes the unmarked cluster fluctuation, with $\bar{n}(L)$ as the mean number density of clusters with luminosity L . As weight we use the cluster X-ray luminosity, $w_i \equiv L_i/\bar{L}$, where \bar{L} is the first sample moment (or mean) of the luminosity in the sample. Note that by definition $\bar{w} = 1$, which in turn implies that $\bar{n}_w = \bar{w}\bar{n} = \bar{n}$. The quantity $n_w(\mathbf{r}; L)$ denotes a inhomogeneous marked point-process, in which two sources of stochasticity are present, namely, the associated to the sampling process giving rise to the observed $n(\mathbf{r}; L)$, and that due to the stochastic nature of the marks. We assume that the halo distribution $n(\mathbf{r}, L)$ is the result of an inhomogeneous Poisson point process³ (e.g. Peebles 1980).

The weighted haloes are embedded into a 380^3 cubic grid using a cloud-in-cell mass assignment scheme (Hockney & Eastwood 1988). We use the FFTW algorithm (Frigo & Johnson 2012) to compute the Fourier transform of $\delta_w(\mathbf{r}; L)$, $\tilde{\delta}_w(\mathbf{k}; L)$, correcting thereafter for aliasing effects (see e.g. Angulo et al. 2008). We next obtain estimates⁴ of the unmarked $P(k; L)$, the cross power spectrum between the unweighted and weighted halo density fields $\mathcal{W}_1(k; L)$ and the luminosity-weighted power spectrum $\mathcal{W}_2(k; L)$ by

$$\hat{P}(k_i; L_j) = \langle |\tilde{\delta}_h(\mathbf{k}; L_j)|^2 \rangle_{k_i} - \frac{1}{\bar{n}(L_j)}, \quad (3)$$

³ Strictly speaking, a Poisson model cannot properly describe the distribution of galaxy clusters as these objects are subject to the so-called halo exclusion effects (e.g. Porciani & Gialvalisco 2002; Tinker et al. 2005; Smith et al. 2007). Exclusion arises due to the fact that haloes have finite sizes. This implies that $\xi(r) \rightarrow -1$ on scales below the minimum scale probed by the halo catalog. For an ideal sample of spherical haloes, such scale equals twice the radius of the smaller halo.

⁴ We denote by \hat{f} the estimates of the quantity f .

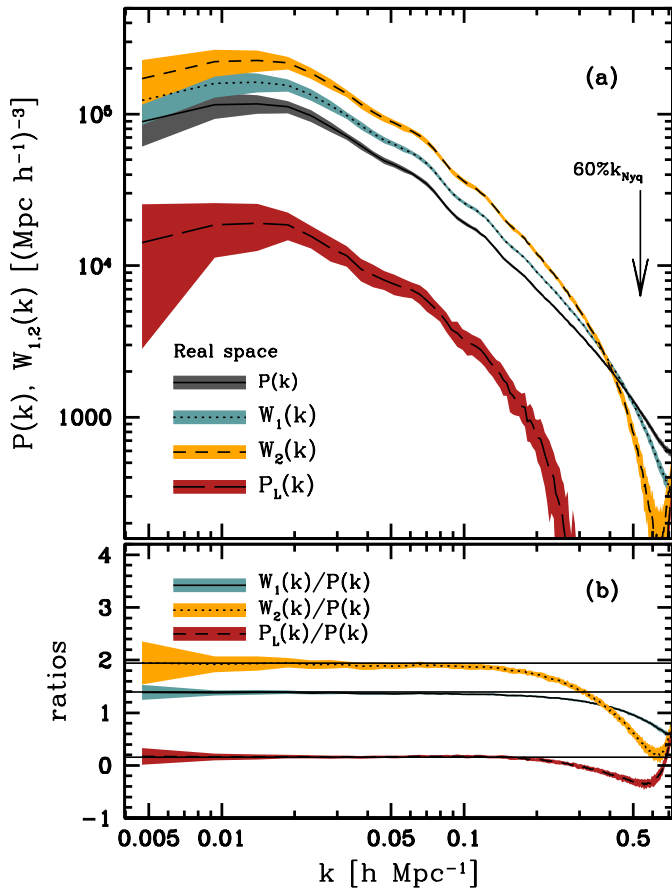


Fig. 1. (a) Mean power spectra $\hat{P}(k)$, $\hat{\mathcal{W}}_{1,2}(k)$ and $\hat{P}_L(k)$ (defined in Sect. 2.2) obtained from the ensemble of N-body simulations, for galaxy clusters within the full luminosity range as described in the text. The 60% of the Nyquist frequency is marked with an arrow. (b) Ratio between the spectra $\hat{\mathcal{W}}_{1,2}(k)$ and $\hat{P}_L(k)$ to the cluster power spectrum $\hat{P}(k)$. Spectra are shown in real space. The horizontal lines show the large-scale predictions discussed in Appendix A. In all panels the shaded regions denote the standard deviation obtained from the ensemble of N-body simulations.

$$\hat{\mathcal{W}}_1(k_i; L_j) = \langle \text{Re}(\tilde{\delta}_h(\mathbf{k}; L_j) \tilde{\delta}_w^*(\mathbf{k}; L_j)) \rangle_{k_i} - \frac{\bar{w}_j}{\bar{n}(L_j)}, \quad (4)$$

$$\hat{\mathcal{W}}_2(k_i; L_j) = \langle |\tilde{\delta}_w(\mathbf{k}; L_j)|^2 \rangle_{k_i} - \frac{\bar{w}_j^2}{\bar{n}(L_j)}, \quad (5)$$

where $\langle \cdot \rangle_{k_i}$ denotes average in spherical shells of width $\Delta k = 2\pi V^{-1/3}$ centered at k_i . The second term in Eq. (3) corresponds to the Poisson shot-noise correction (e.g. Peebles 1980), an extra-variance of the halo field induced by discreteness. Similarly, the extra variance in Eqs. (4) and (5) are the product of the variance related to the Poisson point-like process, and that induced by the luminosity distribution. The term \bar{w}_j^2 denotes the second sample moment of the weights within the j^{th} luminosity bin. Note again that in Eq. (4), $\bar{w}_j = 1$.

Along with the measurements in real space, we also carry out the measurements of two-point statistics in redshift space by means of the distant-observer approximation, i.e., shifting the position of dark matter haloes along the x -axis $x \rightarrow x + v_x/H_0$ where v_x is the x -component of the peculiar velocity of the halo center of mass. We keep Fourier modes up to a $\sim 60\%$ of the

Nyquist frequency $k_{\text{Ny}} = 0.89 h \text{ Mpc}^{-1}$, where the corrections due to the assignment scheme are accurate (e.g. Cole et al. 2005).

In panel (a) of Fig. 1 we show the mean of the real-space power spectra $\hat{P}(k)$ and $\hat{\mathcal{W}}_{1,2}(k)$ (computed using the full luminosity range) with the corresponding standard deviation obtained from the ensemble of realizations of the L-BASICC simulations. At first glance, the estimates of marked power spectra $\hat{\mathcal{W}}_{1,2}(k)$, behave as scaled versions of $\hat{P}(k)$. Indeed, on large scales ($k \lesssim 0.04 h \text{ Mpc}^{-1}$), the ratios $\hat{\mathcal{W}}_{1,2}(k)/\hat{P}(k)$ are well described by a constant factor, as is shown in panel (b) of the same figure. This suggests that the amplitude of the marked power spectra $\hat{\mathcal{W}}_{1,2}(k)$ can be explained, as a first approximation, by including the information of the scaling relation within a sort of luminosity bias (see Appendix A). A more careful analysis reveals, though, a slow decrease of the ratios $\hat{\mathcal{W}}_{1,2}(k)/\hat{P}(k)$ on scales $k \gtrsim 0.04 h \text{ Mpc}^{-1}$ (similarly present in redshift space). Given the error bars, this feature can be regarded as a 1σ deviation from a scale-independent behavior. However, on smaller scales ($k \gtrsim 0.1 h \text{ Mpc}^{-1}$), this trend becomes statistically significant. Note that $\hat{\mathcal{W}}_{1,2}(k)$ and $\hat{P}(k)$ are equally affected by exclusion effect (i.e., they are estimated from the same sample and thus the smallest populated bin of separation is the same, albeit differently weighted)⁵ as well as by the same scale-dependent halo-mass bias (see e.g. Tinker et al. 2005). Therefore, the scale-dependency of the ratios $\hat{\mathcal{W}}_{1,2}(k)/\hat{P}(k)$ is likely to be a signature of the distribution of the weights $w_i w_j$ within pairs at different separations. This suggests that the shape of the luminosity-weighted power spectrum is sensitive to the scaling relation $\mathcal{P}(L|M)$. This will be explored in Sect. 3.

As an attempt to isolate the signal of the clustering of the X-ray luminosity from the unmarked power spectrum, let us define $\delta_L(\mathbf{r}; L) \equiv \delta_w(\mathbf{r}; L) - \delta_h(\mathbf{r}; L) = (n_w(\mathbf{r}; L) - n(\mathbf{r}; L))/\bar{n}(L)$. This fluctuation has zero mean, $\langle \delta_L(\mathbf{k}; L) \rangle = 0$, and variance $P_L(k; L) \equiv \langle |\tilde{\delta}_L(\mathbf{k}; L)|^2 \rangle$, where $\langle \cdot \rangle$ denotes average over an ideal ensemble of realizations. We refer to this variance as the *luminosity power spectrum*. So defined, the variable δ_L accounts for the fluctuations of the weighted number density with respect to the unweighted number density. Since by construction both number densities share the same mean value, this simple subtraction avoids us having to use the observed mean number density as the true mean density, and thus, the estimates of the luminosity power spectrum are free of the so-called integral constraint (e.g., Peacock & Nicholson 1991). The mean number density \bar{n} only enters in the definition of δ_L as a normalization factor. Therefore, the possible difference between the observed and true number density would equally affect all Fourier modes in $P_L(k; L)$ by some constant factor.

The estimates of the luminosity power spectrum are obtained following the same procedure described above, namely, a shell-average of the estimate $|\tilde{\delta}(\mathbf{k}; L)|^2$ with a shot-noise correction S_L :

$$\hat{P}_L(k_i; L_j) = \langle |\tilde{\delta}_L(\mathbf{k}; L_j)|^2 \rangle_{k_i} - S_L. \quad (6)$$

According to the definition of $\delta_L(\mathbf{r})$, the luminosity power spectrum can be written as the combination of the luminosity-weighted power spectra $P_L = \mathcal{W}_2 - 2\mathcal{W}_1 + P$. Thus, we can identify the shot-noise correction with $S_L = \sigma_{w_j}^2/\bar{n}(L_j)$, where $\sigma_{w_j}^2 = \bar{w}_j^2 - 1$. Panel (a) of Fig. 1 shows the mean of the esti-

⁵ By checking the ratio $P(k)/P_{\text{mat}}(k)$, where $P_{\text{mat}}(k)$ is the matter power spectrum measured from the N-body simulations, we see that exclusion dominates the signal of $P(k)$ —measured in the full luminosity range—on scales smaller than $\sim 0.2 h \text{ Mpc}^{-1}$. For the estimates in redshift space, this value shifts to $\sim 0.26 h \text{ Mpc}^{-1}$.

mates of $P_L(k)$ as determined from the ensemble of N-body simulations (in the full luminosity range), together with its standard deviation. On large scales, the shape of $\hat{P}_L(k)$ can be understood as a biased halo power spectrum, i.e., $P_L(k)/P(k) \sim \text{constant}$, prevailing even on intermediate scales ($\sim 0.1 h \text{ Mpc}^{-1}$). In view of the results shown in Appendix A, the luminosity power spectrum can be seen as a directly probing the mean scaling relation. The advantage of directly measuring $P_L(k)$, instead of inferring it from the combination of the spectra $P, \mathcal{W}_{1,2}$, is on the one hand practical, since we would only need to measure only *one* spectrum, instead of three (with their corresponding covariance matrices). On the other hand, the direct assessment of the luminosity power spectrum from a complete sample does not demand random catalogs (needed in the case of samples defined by non-trivial selection functions) *only when the shot-noise contribution is not to be subtracted and only if the shape of $P_L^{ns}(k)$ is to be studied*

2.3. Two-point statistics as probe for cluster scaling relations

Generally we can extract information related to the parameters of a model explaining the observed two-point statistics in three different ways, namely, *i*) using the amplitude of the clustering signal, *ii*) using its full shape (e.g. Sánchez et al. 2012), or *iii*) isolating particular features such as the position of the baryonic acoustic peak in the correlation function or the turn-over in the power spectrum (e.g. Reid et al. 2010; Poole et al. 2013). We will study the information content in cases *i*) and *ii*), and leave for future studies the assessment of the dependence of particular features, e.g., the acoustic peak in the correlation function, on the cluster scaling relations.

2.3.1. Amplitude

The information contained in the amplitude of the clustering signal can be extracted by defining ratios of spectra with respect to the underlying matter power spectrum, or in a less model-dependent fashion, with respect to the clustering of the same population of objects at a given luminosity (e.g. Norberg et al. 2002). As suggested by the panel (b) of Fig. 1, such ratios are approximately scale-independent on large scales (e.g. $k \lesssim 0.04 h \text{ Mpc}^{-1}$). Let us define, for each realization $q = 1, \dots, N$, the following ratios:

$$\begin{aligned} r_1^{(q)}(k_i; L_j) &\equiv \left(\frac{\hat{P}^{(q)}(k_i; L_j)}{\hat{P}^{(q)}(k_i; L_{\text{ref}})} \right)^{\frac{1}{2}}, & r_2^{(q)}(k_i; L_j) &\equiv \left(\frac{\hat{\mathcal{W}}_1^{(q)}(k_i; L_j)}{\hat{\mathcal{W}}_1^{(q)}(k_i; L_{\text{ref}})} \right)^{\frac{1}{2}}, \\ r_3^{(q)}(k_i; L_j) &\equiv \left(\frac{\hat{\mathcal{W}}_2^{(q)}(k_i; L_j)}{\hat{\mathcal{W}}_2^{(q)}(k_i; L_{\text{ref}})} \right)^{\frac{1}{2}}, & r_4^{(q)}(k_i; L_j) &\equiv \left(\frac{\hat{\mathcal{W}}_1^{(q)}(k_i; L_j)}{\hat{P}^{(q)}(k_i; L_j)} \right)^{\frac{1}{2}}, \\ r_5^{(q)}(k_i; L_j) &\equiv \left(\frac{\hat{\mathcal{W}}_2^{(q)}(k_i; L_j)}{\hat{P}^{(q)}(k_i; L_j)} \right)^{\frac{1}{2}}, & r_6^{(q)}(k_i; L_j) &\equiv \left(\frac{\hat{P}_L^{(q)}(k_i; L_j)}{\hat{P}^{(q)}(k_i; L_{\text{ref}})} \right)^{\frac{1}{2}}, \\ r_7^{(q)}(k_i; L_j) &\equiv \left(\frac{\hat{P}_L^{(q)}(k_i; L_j)}{\hat{P}^{(q)}(k_i; L_j)} \right)^{\frac{1}{2}}. \end{aligned} \quad (7)$$

Our set of large-scale luminosity dependent observables is then defined as $r_v^q(L_j) \equiv \langle r_v^q(k_i; L_j) \rangle_{\delta k}$, where $\langle \cdot \rangle_{\delta k}$ denotes the average over wavenumbers in the range $\delta k = [0.01, 0.04] h \text{ Mpc}^{-1}$. The first three probes $r_{1,2,3}(L)$ are defined as ratios of a given power spectrum in different luminosity bins with respect to the same statistics, the latter measured in a fixed (reference) lu-

minosity bin L_{ref} , providing thereby estimates of *relative biases* of the marked spectra. The ratios $r_{4,5}(L)$ are instead defined with respect to the unmarked power spectrum in the same luminosity bin, and we refer to these as estimates of *absolute bias*⁶. Similarly, the ratios $r_{6,7}(L)$ are estimates of relative and absolute bias extracted from the luminosity power spectrum. In these expressions L_{ref} is taken as containing the value $L_\star = 0.63 \times 10^{44} \text{ erg s}^{-1} h^{-2}$, the typical X-ray luminosity of galaxy clusters up to redshift $z \sim 0.2$ (Balaguera-Antolínez et al. 2012). We have checked that our results do not change substantially when other values of L_{ref} are used, except for the high luminosity bins, wherein the clustering estimates display a low signal-to-noise ratio. In Appendix A we show the theoretical predictions for these ratios.

2.3.2. Full shape

The measurements of the luminosity weighted power spectrum shown in Sect. 2.2 revealed that the scaling relation $\mathcal{P}(L|M)$ not only affects the amplitude of the weighted power spectra $\mathcal{W}_{1,2}(k)$, but can also play a role in shaping their broad-band signal. In order to quantify the information encoded in the full shape of the measured spectra $P(k)$, $\mathcal{W}_{1,2}(k)$ and $P_L(k)$, we use their estimates in the range of wave numbers $0.02 \leq k/(h \text{ Mpc}^{-1}) \leq 0.2$, with $\tilde{N}_k = 32$ Fourier modes, and using the full X-ray luminosity range.

As pointed out in Sect. 2.2, the variance of the fluctuations of the luminosity-weighted and luminosity power spectrum has a contribution which embodies two forms of randomness: one associated to the finite number of haloes, and other related to the distribution of the marks with respect to its mean. These two effects are represented by Eq.(6). The shot-noise subtraction in the power spectrum of galaxy clusters is a delicate issue. Clusters, being rare objects, display number densities sufficiently low to generate a shot-noise contribution that can be traceable even on the largest scales. As an example of its relevance, it can be seen that estimates of power spectra without shot-noise correction can generate a scale dependent bias on scales where the ratios between corrected spectra were fairly described by a constant factor (see e.g. Pollack et al. 2012). Strictly speaking, not subtracting the shot-noise correction from the estimates of power spectra is not an off base procedure, given the fact that this correction is a model in itself, and as such, can be included in the modeling of the clustering signal. In order to assess the impact of the shot-noise correction in the amount of information we can retrieve, below we will consider the case in which the information content from the luminosity power spectrum is extracted from its shot-noise uncorrected estimate, which we denote by P_L^{ns} .

3. Information content

In this section we quantify the amount of information that our clustering-related observables contain regarding the mass-X ray luminosity scaling relation. Before we proceed, let us recall that in the context of galaxy cluster experiments, one-point statistics –such as cluster number counts– represent the standard probe for cosmological parameters and scaling relations (e.g. Lima & Hu 2004; Cunha & Evrard 2010; Pillepich et al. 2012). In order to compare our results, which are based on two-point statistics, with a one-point statistics probe, we use the X-ray luminosity function (XLF hereafter) measured in $\tilde{n}_\ell = 25$ equally

⁶ We mean absolute with respect to the unmarked cluster power spectrum, not with respect to the matter power spectrum.

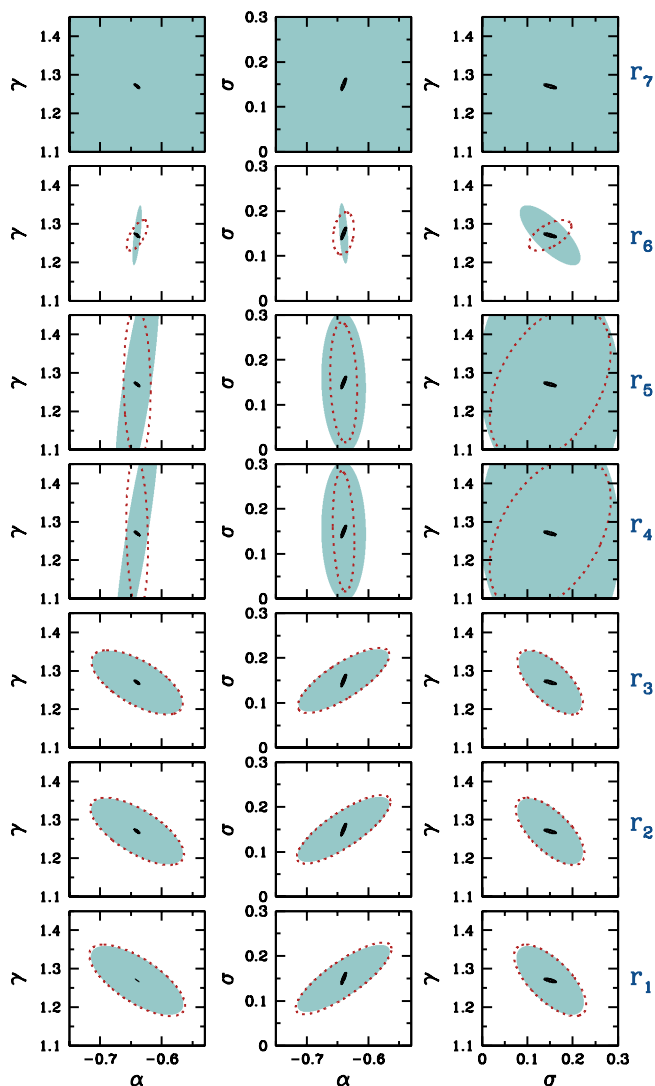


Fig. 2. Joint 1σ error ellipses for the parameters $\{\alpha, \gamma, \sigma\}$ of the scaling relation $\mathcal{P}(L|M)$, obtained from the Fisher-matrix analysis in real (shaded area) and redshift space (dotted lines contours), using as observables the set $r_{\nu=1,\dots,7}(L)$ defined in Eq. (7). The small filled contours represent the results using the XLF.

log-spaced bin, and denoted by $\hat{\Phi}(L)$. Given the fact that the cosmological parameters are kept fixed throughout the analysis⁷, the information content in the XLF can provide a fair level of comparison to assess the capability of the clustering probes in retrieving information on the cluster scaling relation against the standard procedures. Our set of observables is summarized as

$$\mu_j^q = \{r_{\nu=1,\dots,7}(L_j), \hat{P}(k_j), \hat{W}_{\nu=1,2}(k_j), \hat{P}_L(k_j), \hat{\Phi}(L_j)\}, \quad (8)$$

where the index j runs from $(1, \dots, n_\ell)$ for the ratios $r_\nu(L)$, $(1, \dots, \tilde{N}_k)$ for the power spectra and $(1, \dots, \tilde{n}_\ell)$ for the XLF. For each observable, its mean $\bar{\mu}$ and covariance matrix \mathbf{C} are respectively given by $\bar{\mu}_i = \langle \mu_i \rangle_{\text{ens}}$ and $C_{ij} = \langle \mu_i \mu_j \rangle_{\text{ens}} - \bar{\mu}_i \bar{\mu}_j$, where $\langle \cdot \rangle_{\text{ens}}$ denotes averages over the ensemble of realizations of the L-BASICC simulations.

We carry out a Fisher-matrix analysis (e.g. Tegmark et al. 1997). The Fisher matrix represents the ensemble average of the

⁷ Even though the dependence on cosmological parameters of the cluster number counts and luminosity function is slightly different, their dependence on the parameters of the scaling relation is the same.

Hessian of the natural logarithm of the likelihood function of a data set given a model, and its customary application aims to forecast uncertainties of a set of model parameters from a given experiment. Our approach is slightly different, though, since we aim to quantify the sensitivity of each of the observables defined in Eq. (8) to the set of parameters $\{\mathcal{X}\}$ using their measurements and covariance matrices directly extracted from the simulations. In other words, we assume a perfect knowledge of model and covariance for our observables. Under the assumption that the observables are drawn from a Gaussian distribution, the elements of the Fisher matrix \mathbf{F} are written as

$$F_{xy} = \frac{1}{2} \text{Tr} \left[\mathbf{C}^{-1} \mathbf{C}_{,x} \mathbf{C}^{-1} \mathbf{C}_{,y} + \mathbf{C}^{-1} \left(\bar{\mu}_{,x} \bar{\mu}_{,y}^T + \bar{\mu}_{,y} \bar{\mu}_{,x}^T \right) \right] \Big|_{x=y=x_{\text{fid}}}, \quad (9)$$

where $,x \equiv \partial/\partial x$ and x_{fid} denote the fiducial values of the parameters $\{\mathcal{X}\}$, defined in Sect. 2.1. The covariance matrix of the parameters of the model is $C_{xy} \approx F_{xy}^{-1}$, and the marginal error of each parameter is obtained from the Cramér-Rao inequality $\sigma_x \geq (\mathbf{F}^{-1})_{xx}^{1/2}$. We used a double-side variation in order to accurately estimate the derivatives with respect to the parameters. This leads us to the computation of $27(\text{models}) \times 50(\text{realizations}) \times 2(\text{real and redshift-space estimates}) \times 3(\text{marked spectra}) \times 10(\text{luminosity bins}) = 8.1 \times 10^5$ estimates of power spectrum.

Three key aspects of our Fisher matrix analysis are considered for our analysis. Firstly, by means of the so-called D’Agostino’s K2 goodness-of fit test, we have verified that the distribution of the observables defined in Eq. (8) within the suite of realizations of the N-body simulations is compatible to a 95 per cent confidence with a normal distribution within the ranges of X-ray luminosity and wavenumbers of interest. Secondly, we note that when computing the Fisher matrix for all our observables (with mean values $\bar{\mu} \neq 0$), we omit the term containing the derivatives of the covariance matrix, since it adds spurious information that considerably shrinks the marginalized errors (Carron 2013).

Finally, when exploring the information content encoded solely in the shape of the power spectra, we treat the amplitude of the mean spectra as a nuisance parameter. Under the assumption that these amplitudes have flat or Gaussian-distributed priors, analytical marginalization of the covariance matrix over these parameters is possible (e.g. Lewis & Bridle 2002; Taylor & Kitching 2010). For a flat prior on these amplitudes, the inverse of the marginalized covariance matrix is obtained by subtracting the factor $(\mathbf{C}^{-1} \bar{\mu}^T \bar{\mu}) / (\text{Tr}[\bar{\mu} \mathbf{C} \bar{\mu}^T])$ from the original inverted covariance matrix.

We quantify the information obtained from each of our observables by a figure-of-merit (FoM hereafter) defined as the inverse of the area of the marginalized 68% error ellipse of each pair of parameters. We also compute the total FoM given by the volume of the three-dimensional 68% error ellipsoid. We present the results from the Fisher matrix analysis in Figs. 2 and 3. Figure 4 condenses the FoM derived from our set of observables. We will draw our conclusions based in three figures.

3.1. Information content in the amplitude

Figure 2 shows the joint 1σ error ellipses obtained from the Fisher-matrix analysis of the set $r_{\nu=1,\dots,7}(L)$. The results are presented in real and redshift space. We next draw some conclusions based on this figure, in conjunction with Fig. 4.

- The sensitivity to the parameters of the scaling relation varies little between the observables $r_{1,2,3}(L)$. This is also true when

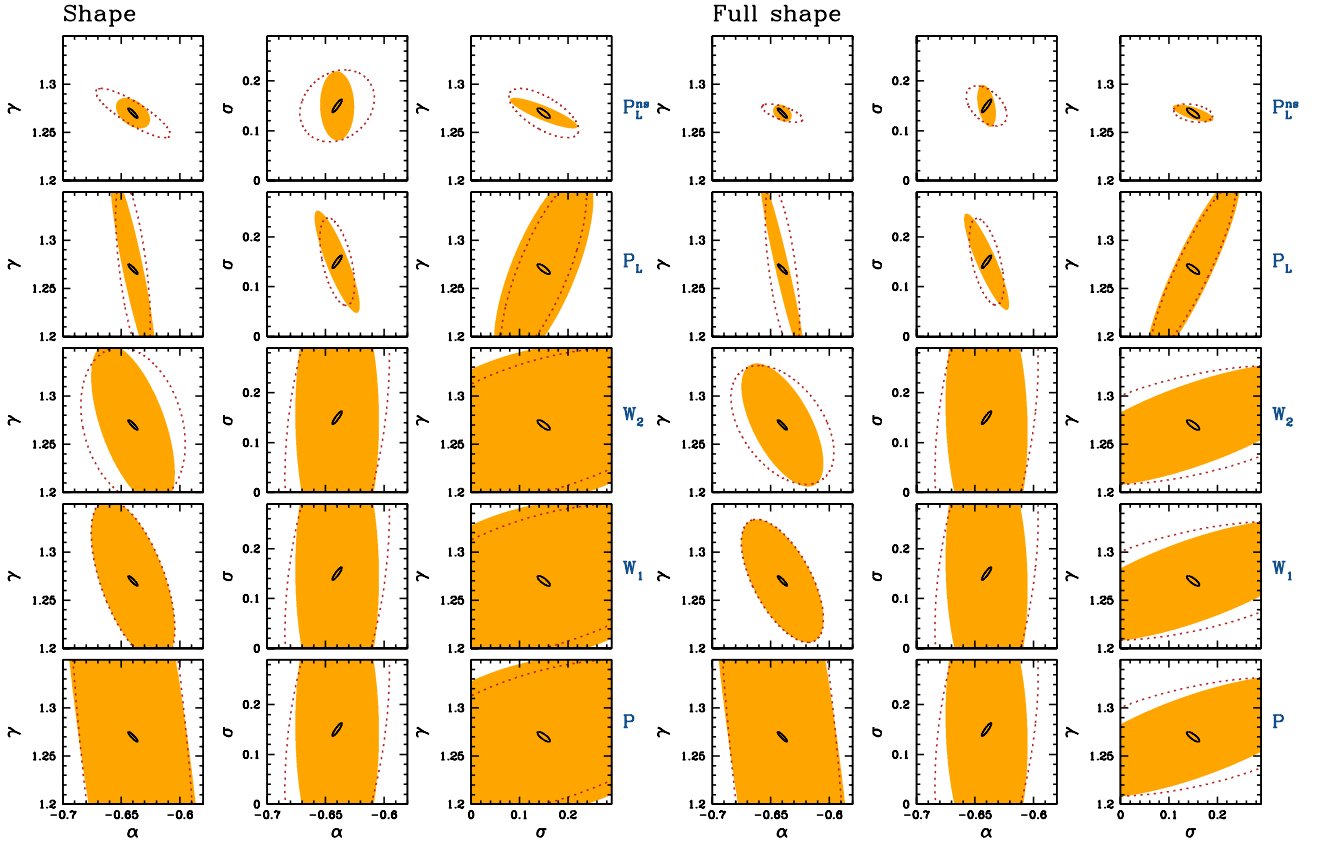


Fig. 3. Joint 1σ error ellipses for the parameters $\{\alpha, \gamma, \sigma\}$ of the scaling relation $\mathcal{P}(L|M)$, obtained from the Fisher-matrix analysis of power spectra $P(k)$, $\mathcal{W}_{1,2}(k)$ and $P_L(k)$ defined in Sect. 2.2. P_L^{ns} denotes the shot-noise uncorrected estimates of the luminosity power spectrum. Results are shown in real (shaded area) and redshift space (dotted lines). The estimates of these spectra are obtained within the full-luminosity range and using Fourier modes in the interval $0.02 < k/(h\text{Mpc}^{-1}) < 0.2$. The solid contours represent the results using the XLF. Right panel shows the results using after marginalizing over the amplitude of the power spectra. Left panel shows the results using the full-shape.

these observables are measured in redshift space. The estimates associated of absolute biases $r_{4,5}(L)$ are slightly more sensitive to the signal of the spectra in redshift space.

- When the ratios are defined with respect to the unmarked power spectrum (i.e., $r_{4,5}(L)$), the marginalized errors on the amplitude, σ_α , decrease while σ_γ increases, with a net decrease in the total FoM. Therefore, the set $r_{1,2,3}(L)$ proves to be more sensitive to the set $\{\gamma, \sigma\}$, while the set $r_{4,5}(L)$ sets tighter constraints on the amplitude α .
- The estimates of relative bias extracted from the luminosity power spectrum $r_6(L)$, generate FoM that are approximately two orders of magnitude above those obtained from the luminosity weighted power spectrum, say $r_3(L)$, marking a noticeable improvement. The total FoM of derived from this probe is only ~ 40 times below that derived from the XLF. On the other hand, the estimate of absolute bias $r_7(L)$ sets poor constraints.
- In general, better constraints are obtained from the estimates of relative bias. As pointed out before, the selection of the reference luminosity does not affect our conclusions, except for very high values of L_{ref} .

We conclude that, regarding the amplitude of the cluster power spectrum, the unmarked analysis is accurate enough and no extra-information is gained by measuring the luminosity dependence of the amplitude of the luminosity-weighted power spectrum. On the other hand, we have shown that the estimates of luminosity bias obtained from the luminosity power spectrum, $r_6(L)$, allows us to retrieve an amount of information on the scal-

ing relation which is only one order of magnitude below that characterizing the XLF.

3.2. Information content in the full shape

Figure 3 shows the error ellipses from the analysis of the full shape of the power spectra $\hat{P}(k)$, $\hat{\mathcal{W}}_{1,2}(k)$, $\hat{P}_L(k)$ and $\hat{P}_L^{\text{ns}}(k)$, both in real and redshift space, with Fourier modes in the range $0.02 < k/(h\text{Mpc}^{-1}) < 0.2$. The left panel in that figure corresponds to the results obtained after marginalizing the covariance matrix of each observable with respect to an overall amplitude, while the right panel shows results obtained after using the information encoded in the full shape. This figure confirms the intuitive prediction that more information (smaller error ellipses) is gained when the full shape is used in the analysis. The content of information retrieved from the luminosity power spectrum stands as the most sensitive probe.

Let us complement the information shown in Fig. 3 with the information shown in Fig. 4. From these we conclude the following:

- The marked power spectra $\hat{\mathcal{W}}_{1,2}(k)$ generates higher FoM compared to $P(k)$, due mainly to their sensitivity to the slope of the scaling relation γ . These three spectra are almost equally sensitive to the intrinsic scatter σ and the amplitude α .
- A gain of information content on the scaling relation is obtained from the luminosity power spectrum, with FoM increased approximately by an order of magnitude with respect

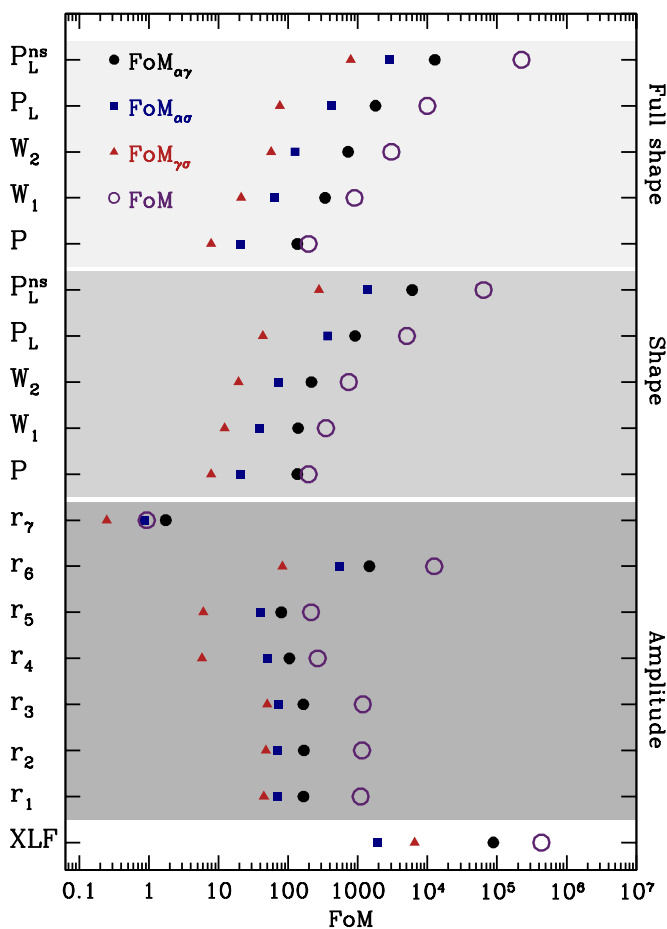


Fig. 4. Figures-of-merit obtained from the 1σ error ellipses of each pair of parameters of the scaling relation, taken from the different observables μ_j defined in Eq. (8). With FoM we denote the figure-of-merit computed as the volume of the 3-dimensional 68% error ellipsoid. To facilitate the understanding of this figure, the dark gray, gray and light gray areas denote observables accounting for the amplitude, the shape and the full shape of power spectra respectively. Results are shown in real space. Noticeably, the luminosity power spectrum P_L proves to provide more information regarding the scaling relation than the luminosity-weighted spectra. Furthermore, the estimates of luminosity power spectrum without shot-noise correction generates FoM comparable to those obtained from the analysis of the XLF.

to that obtained with \mathcal{W}_2 , or, ~ 40 times below that characterizing the information encoded in the XLF.

- We carried out analysis using the shot-noise uncorrected estimates of the power spectra. As a result, the FoM obtained are higher than those presented in Fig. 4, as has been explicitly portrayed for the case of $P_L(k)$. The total FoM obtained from $P_L^{ns}(k)$ is a factor ~ 2.5 smaller than the corresponding value obtained from the XLF, which is noticeable if we compare it to the factors ~ 15 and $\sim 2 \times 10^3$ derived from $\mathcal{W}_2(k)$ and $P(k)$ respectively⁸. The ratios between the FoM obtained from the non-corrected estimates to those derived from the corrected ones (using their full shape as probes) are $\sim 3, 21, 23$ for P, \mathcal{W}_2 and P_L respectively, illustrating how sensitive the clustering signal of galaxy clusters to the shot-noise correction is.

⁸ Note that the Fisher matrix of P_L is *not* the sum of the Fisher matrix of the weighted spectra.

Summarizing, Fig. 4 attempts to answer the question posed by the title of this paper. The improvement in the FoM obtained from the luminosity power spectrum with respect to the standard probes (i.e., unweighted clustering analysis) represents the main result of our analysis.

4. Discussion and conclusions

In this paper we aimed at exploring the capability of the so-called marked-statistics of galaxy clusters to retrieve information on describing the links between cluster masses and cluster X-ray luminosities. To this end, we assigned X-ray luminosities to dark matter haloes in a suite of N-body simulations and measured luminosity-weighted power spectra $\mathcal{W}_{1,2}(k)$ and luminosity power spectrum $\hat{P}_L(k)$, defined in Sect. 2.2. The luminosity power spectrum has been defined such that it directly measures the clustering of X-ray luminosity.

We extracted the information related to the scaling relation by dissecting the clustering signal in three different parts: first, we isolated the large scale information of the power spectra measured in different luminosity bins, and measured estimates of luminosity bias. Second, we explored the information encoded in the shape of the clustering signal and third, we considered their full shape (i.e., shape and amplitude). This yields a total of twelve observables. By carrying out a Fisher matrix analysis, we quantified the amount of information regarding the cluster scaling relation from each of these observables through the definition of a Figure of Merit (FoM). In terms of the amplitude, we showed that the information encoded in the estimates of cluster luminosity bias measured from the unweighted power spectrum is close to that obtained from the bias of the weighted spectra, and hence no sensitive gain of information is achieved in terms of the amplitude. However, a relevant increase in the information content is achieved when estimates of relative bias are extracted from the luminosity power spectrum, reaching FoM that are only one order of magnitude below the values derived from the XLF analysis. Similarly, when exploring the information content within the full shape of power spectra, we found that that in $P_L(k)$ overcomes the amount of information contained in the spectra $\mathcal{W}_{1,2}(k)$ and $P(k)$. This gain of information obtained from the estimates of the luminosity power spectrum, when compared to the weighted spectra and the XLF, represents the main result of this paper. Consequently, we suggest the mining of this probe in order to extract information of cluster underlying scaling relations (and cosmological parameters) from future galaxy cluster experiments.

An obvious question arises, regarding the feasibility of the clustering signal to set precise constraints on cluster scaling relations in future galaxy cluster surveys. From the observational point of view, the volume of the N-body simulations we have used to create cluster catalogs mimics that of a full-sky complete sample to a maximum redshift of $z \sim 0.3$. The resulting mean number density resembles that expected from the *eROSITA* experiment (Pillepich et al. 2012). Therefore the precision to which *only* the scaling relation could be constrained from these forthcoming samples -when redshifts are available and using $P_L(k)$ - can be of the same order as that obtained from our analysis. On the other hand, the volumes which will be probed by the forthcoming surveys will generate statistical errors on the estimates of power spectra that might be compatible to the systematic errors present in the modeling of clustering. This situation is especially noticeable on small scales – probed by a large number of modes – where the clustering signal is dominated by the non-linear evolu-

tion of the cluster matter density field, the scale-dependent halo-mass bias, the halo exclusion and ultimately baryonic effects.

From a theoretical perspective, the fact that we have considered estimates of the clustering signal up to scales of $k \lesssim 0.2 h \text{ Mpc}^{-1}$ could be a point of concern. On these scales, highly complex processes (e.g. non-linear evolution of the matter density field, scale-dependent halo biasing and halo exclusion effect) become non-negligible. In the last two decades, a major progress in the understanding of some of these processes has been accomplished. In that regard, there are a number of attempts to describe the non-linear evolution of dark matter, either based on numerical fits to N-body simulations (e.g. Peacock & Dodds 1996; Smith et al. 2003) as well as theoretical predictions (e.g. Bernardeau et al. 2002; Crocce & Scoccimarro 2006; McDonald 2007; Matsubara 2011). The link between dark matter and haloes –the halo-mass bias– has been also an active area of research, regarding its nature and fitting formulae for its implementation (see e.g. Porciani 2013, for a recent review on this subject). Even if these theoretical predictions accurately describe the results from N-body simulations, baryonic effects within galaxy clusters (e.g. radiative cooling, star formation, feedback mechanism due to AGN and Supernova) can severely spoil the expectations of modeling the observed clustering signal to the accuracy achieved by state-of-the-art cosmological simulations of dark matter. Indeed, such effects have been shown to substantially modify the abundance and clustering of clusters with respect to pure dark matter-based predictions (e.g. Stanek et al. 2009; Rudd et al. 2008; van Daalen et al. 2011; Cui et al. 2012; Balaguera-Antolínez & Porciani 2013). In view of the plethora of models accounting for the baryonic effects that shape the intra-cluster medium, and the small scales (astrophysical, instead of cosmological) where these effects take place, a precise modeling of the abundance and clustering of galaxy clusters based on N-body simulations is still far from being achieved. Even though it is out of the scope of this paper to discuss the impact of the systematics present in the modeling of the quantities mentioned above, we recognize their relevance in order to extract accurate information regarding the parameters describing the observed clustering pattern of galaxy clusters (especially using the luminosity power spectrum) from forthcoming galaxy and galaxy cluster surveys such as *eROSITA*, DES (The Dark Energy Survey Collaboration 2005) or Euclid (Laureijs et al. 2011). We notice that the only explicit model that we have assumed in our analysis is that the halo distribution behaves like a Poisson point process, which is a debatable assumption (see e.g., Casas-Miranda et al. 2002; Smith et al. 2007).

The weighted two-point statistics proves to be a powerful tool to characterize explicit dependence upon cluster intrinsic properties of the clustering of galaxy clusters. The implementation of this statistics, either in Fourier space (as we have shown in this paper) or in configuration space (see e.g. Sheth 2005), can contribute to set tight constraints on the parameters that characterize the physics of the intra-cluster medium, interestingly intertwining cosmology and astrophysics at the galaxy cluster-scale.

Acknowledgments I am grateful to Raúl Angulo for making available the L-BASICC II simulations. I thank Cristiano Porciani and Nina Roth for the useful discussions and suggestions that helped to improve the presentation and content of the manuscript. I acknowledge support through the SFB-Transregio 33 “The Dark Universe” by the Deutsche Forschungsgemeinschaft (DFG).

References

- Allen, S. W., Evrard, A. E., & Mantz, A. B. 2011, *Annu.Rev.Astro.Astrophys.*, 49, 409
- Angulo, R. E., Baugh, C. M., Frenk, C. S., & Lacey, C. G. 2008, *MNRAS*, 383, 755
- Balaguera-Antolínez, A. & Porciani, C. 2013, *JCAP*, 4, 22
- Balaguera-Antolínez, A., Sánchez, A. G., Böhringer, H., & Collins, C. 2012, *MNRAS*, 425, 2244
- Balaguera-Antolínez, A., Sánchez, A. G., Böhringer, H., et al. 2011, *MNRAS*, 413, 386
- Bardeen, J. M., Bond, J. R., Kaiser, N., & Szalay, A. S. 1986, *ApJ*, 304, 15
- Bernardeau, F., Colombi, S., Gaztañaga, E., & Scoccimarro, R. 2002, *Phys. Rep.*, 367, 1
- Bianchi, D., Guzzo, L., Branchini, E., et al. 2012, *MNRAS*, 427, 2420
- Böhringer, H., Collins, C. A., Guzzo, L., et al. 2002, *ApJ*, 566, 93
- Carron, J. 2013, *A&A*, 551, A88
- Casas-Miranda, R., Mo, H. J., Sheth, R. K., & Boerner, G. 2002, *MNRAS*, 333, 730
- Cole, S., Percival, W. J., Peacock, J. A., et al. 2005, *MNRAS*, 362, 505
- Cooray, A. & Sheth, R. 2002, *Phys. Rep.*, 372, 1
- Crocce, M. & Scoccimarro, R. 2006, *Phys.Rev.D*, 73, 063519
- Cui, W., Borgani, S., Dolag, K., Murante, G., & Tornatore, L. 2012, *MNRAS*, 423, 2279
- Cunha, C. E. & Evrard, A. E. 2010, *Phys. Rev.D*, 81, 083509
- Finoguenov, A., Reiprich, T. H., & Böhringer, H. 2001, *AA*, 368, 749
- Frigo, M. & Johnson, S. G. 2012, *FFTW: Fastest Fourier Transform in the West*, astrophysics Source Code Library
- Giodini, S., Pierini, D., Finoguenov, A., et al. 2009, *ApJ*, 703, 982
- Hamilton, A. J. S. 1998, in *Astrophysics and Space Science Library*, Vol. 231, The Evolving Universe, ed. D. Hamilton, 185
- Hockney, R. W. & Eastwood, J. W. 1988, *Computer simulation using particles*
- Jenkins, A., Frenk, C. S., White, S. D. M., et al. 2001, *MNRAS*, 321, 372
- Kaiser, N. 1986, *MNRAS*, 222, 323
- Kaiser, N. 1987, *MNRAS*, 227, 1
- Kravtsov, A. V. & Borgani, S. 2012, *Annu.Rev.Astro.Astrophys.*, 50, 353
- Laureijs, R., Amiaux, J., Arduini, S., et al. 2011, *ArXiv e-prints*
- Lewis, A. & Bridle, S. 2002, *Phys.Rev.D*, 66, 103511
- Lima, M. & Hu, W. 2004, *Phys. Rev. D*, 70, 043504
- Mantz, A., Allen, S. W., Ebeling, H., Rapetti, D., & Drlica-Wagner, A. 2010, *MNRAS*, 406, 1773
- Matsubara, T. 2011, *Phys.Rev.D*, 83, 083518
- McDonald, P. 2007, *Phys. Rev. D*, 75, 043514
- Mo, H., van den Bosch, F. C., & White, S. 2010, *Galaxy Formation and Evolution*
- Mo, H. J. & White, S. D. M. 1996, *MNRAS*, 282, 347
- Norberg, P., Baugh, C. M., Hawkins, E., et al. 2002, *MNRAS*, 332, 827
- Peacock, J. A. & Dodds, S. J. 1996, *MNRAS*, 280, L19
- Peacock, J. A. & Nicholson, D. 1991, *MNRAS*, 253, 307
- Peebles, P. J. E. 1980, *The large-scale structure of the universe*
- Pierpaoli, E., Borgani, S., Scott, D., & White, M. 2003, *MNRAS*, 342, 163
- Pillepich, A., Porciani, C., & Hahn, O. 2010, *MNRAS*, 402, 191
- Pillepich, A., Porciani, C., & Reiprich, T. H. 2012, *MNRAS*, 422, 44
- Planck Collaboration, Ade, P. A. R., Aghanim, N., et al. 2013, *ArXiv e-prints*
- Planck Collaboration, Aghanim, N., Arnaud, M., et al. 2011, *AA*, 536, A12
- Pollack, J. E., Smith, R. E., & Porciani, C. 2012, *MNRAS*, 420, 3469
- Poole, G. B., Blake, C., Parkinson, D., et al. 2013, *MNRAS*, 429, 1902
- Porciani, C. 2013
- Porciani, C. & Giavalisco, M. 2002, *ApJ*, 565, 24
- Pratt, G. W., Croston, J. H., Arnaud, M., & Böhringer, H. 2009, *AA*, 498, 361
- Rapetti, D., Blake, C., Allen, S. W., et al. 2013, *MNRAS*
- Rasia, E., Meneghetti, M., Martino, R., et al. 2012, *New Journal of Physics*, 14, 055018
- Reid, B. A., Percival, W. J., Eisenstein, D. J., et al. 2010, *MNRAS*, 404, 60
- Rudd, D. H., Zentner, A. R., & Kravtsov, A. V. 2008, *ApJ*, 672, 19
- Sánchez, A. G., Scóccola, C. G., Ross, A. J., et al. 2012, *MNRAS*, 425, 415
- Sarazin, C. L. 1988, *S&T*, 76, 639
- Schlather, M. 2001, *Bernoulli*, 7, pp. 99
- Schuecker, P., Böhringer, H., Guzzo, L., et al. 2001, *A&A*, 368, 86
- Semboloni, E., Hoekstra, H., & Schaye, J. 2012, *ArXiv e-prints*
- Sheth, R. K. 2005, *MNRAS*, 364, 796
- Sheth, R. K. & Tormen, G. 1999, *MNRAS*, 308, 119
- Skibba, R., Sheth, R. K., Connolly, A. J., & Scranton, R. 2006, *MNRAS*, 369, 68
- Skibba, R. A. & Sheth, R. K. 2009, *MNRAS*, 392, 1080
- Smith, R. E., Peacock, J. A., Jenkins, A., et al. 2003, *MNRAS*, 341, 1311
- Smith, R. E., Reed, D. S., Potter, D., et al. 2012, *ArXiv e-prints*
- Smith, R. E., Scoccimarro, R., & Sheth, R. K. 2007, *Phys. Rev. D*, 75, 063512
- Stanek, R., Evrard, A. E., Böhringer, H., Schuecker, P., & Nord, B. 2006, *ApJ*, 648, 956
- Stanek, R., Rasia, E., Evrard, A. E., Pearce, F., & Gazzola, L. 2010, *ApJ*, 715, 1508
- Stanek, R., Rudd, D., & Evrard, A. E. 2009, *MNRAS*, 394, L11
- Taylor, A. N. & Kitching, T. D. 2010, *MNRAS*, 408, 865
- Tegmark, M., Taylor, A. N., & Heavens, A. F. 1997, *ApJ*, 480, 22
- The Dark Energy Survey Collaboration. 2005, *ArXiv Astrophysics e-prints*
- Tinker, J., Kravtsov, A. V., Klypin, A., et al. 2008, *ApJ*, 688, 709
- Tinker, J. L., Robertson, B. E., Kravtsov, A. V., et al. 2010, *ApJ*, 724, 878
- Tinker, J. L., Weinberg, D. H., Zheng, Z., & Zehavi, I. 2005, *ApJ*, 631, 41
- van Daalen, M. P., Schaye, J., Booth, C. M., & Dalla Vecchia, C. 2011, *MNRAS*, 415, 3649
- Vikhlinin, A., Kravtsov, A. V., Burenin, R. A., et al. 2009, *ApJ*, 692, 1060
- Warren, M. S., Abazajian, K., Holz, D. E., & Teodoro, L. 2006, *ApJ*, 646, 881
- White, M. & Padmanabhan, N. 2009, *MNRAS*, 395, 2381
- Wu, H.-Y., Zentner, A. R., & Wechsler, R. H. 2010, *ApJ*, 713, 856

Appendix A: The cluster-mass bias

The ratios $r_\nu(L)$ defined in Sect. 2.3.1 can be predicted under the assumption that, on large scales, dark matter haloes of a given mass M are biased tracers of the underlying dark matter distribution. In the so-called local bias model, to leading order in perturbation theory (e.g. Cooray & Sheth 2002), this is expressed as $P(k; M) = b^2(M)P_{\text{mat}}(k)$, where $P_{\text{mat}}(k)$ denotes the power spectrum of the dark matter and $b(M)$ is a scale-independent halo-mass bias. Given a halo mass function $n(M)dM$ (i.e., the number of dark matter haloes with masses between M and $M + dM$ per unit comoving volume), a scaling relation $\mathcal{P}(L|M)$ and a selection function $\hat{\phi}(M)$ (i.e., the probability of having a cluster with mass M given some selection criteria), the real-space marked power spectra can be written as $\mathcal{W}_\nu(k, L) = (\tilde{b}_w(L)/\tilde{b}(L))^\nu P(k, L)$ (e.g. Cooray & Sheth 2002; Sheth 2005), where

$$\tilde{b}_w(L) \equiv \frac{\int_0^\infty n(M)\hat{\phi}(M, L)b(M)\langle L|M\rangle dM}{\int_0^\infty n(M)\hat{\phi}(M, L)\langle L|M\rangle dM}, \quad (\text{A.1})$$

and

$$\tilde{b}(L) \equiv \frac{\int_0^\infty n(M)\hat{\phi}(M, L)b(M)dM}{\int_0^\infty n(M)\hat{\phi}(M, L)dM}, \quad (\text{A.2})$$

is the effective cluster-matter bias. For a given bin of X-ray luminosity, the selection function can be expressed as the average of the scaling relation given by Eq. (1) in that luminosity bin. The ratios $r_{1,2,3}(L)$ in real space can be therefore interpreted as estimates of $b(L)/b(L_{\text{ref}})$, $b_w(L)b(L)/(b(L_{\text{ref}})b_w(L_{\text{ref}}))$ and $b_w(L)/b_w(L_{\text{ref}})$ respectively. Also, the information contained in the ratio $r_4(L)$ should be the same as that contained in the ratio $r_5(L)$, since these are estimates of the ratio $(b_w(L)/b(L))^{1/2}$ and $b_w(L)/b(L)$ respectively. Accordingly, the luminosity power spectrum can be written as

$$P_L(k; L) = \left(\frac{\tilde{b}_w(L)}{\tilde{b}(L)} - 1 \right)^2 P(k; L), \quad (\text{A.3})$$

from which the predictions for the ratios $r_{6,7}(L)$ can be readily obtained. Note that, according to Eq. (1), the moments of the luminosity L are linked to the scaling relation via $\langle L^n | M \rangle = \exp(n\langle \ell | M \rangle + \frac{n^2}{2}\sigma^2)$. Therefore, the bias \tilde{b}_w is directly sensitive to the mean of the scaling relation, yet indirectly (only through $\hat{\phi}(M, L)$) of the intrinsic scatter.

The redshift-space estimates of the ratios $r_\nu(L)$ can be similarly obtained. Under the plane-parallel approximation, the large-scale signal of the redshift-space cluster power spectrum $P^s(k, L)$ can be described by the so-called Kaiser effect (e.g. Kaiser 1987; Hamilton 1998) $P^s(k, L) = (1 + 2\beta/3 + \beta^2/5)P(k, L)$ where $\beta \equiv f/\tilde{b}(L)$ and $f \equiv d \ln D(a)/d \ln a$ is the growth index ($D(a)$ is the growth factor) (e.g. Peebles 1980). Given the cosmology and redshift-output of the L-BASICC simulations that we have used, $f = 0.44$. The Kaiser effect can be generalized to the marked power spectra (e.g. Skibba et al. 2006) as

$$\mathcal{W}_1^s(k, L) = \frac{\tilde{b}_w(L)}{\tilde{b}(L)} \left(1 + \frac{1}{3}(\beta + \beta_w) + \frac{1}{5}\beta\beta_w \right) P(k, L), \quad (\text{A.4})$$

and

$$\mathcal{W}_2^s(k, L) = \frac{\tilde{b}_w^2(L)}{\tilde{b}^2(L)} \left(1 + \frac{2}{3}\beta_w + \frac{1}{5}\beta_w^2 \right) P(k, L), \quad (\text{A.5})$$

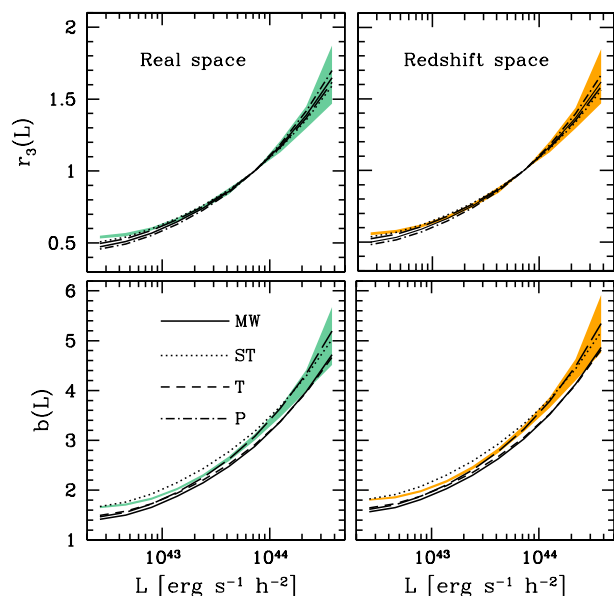


Fig. A.1. The ratio $r_3(L)$ (top panels) defined in Eq. (7), and the luminosity bias $b(L)$ (bottom panels) obtained in the range $0.02 \leq k/(h \text{ Mpc}^{-1}) \leq 0.08$. Results are shown in real (right panel) and redshift (left panel) space. For readability, we only show with shaded regions the standard deviation obtained from the N-body simulations. The solid line represents the predictions presented in Sect. 2.3.1 using expressions for the halo-mass bias as reported by different authors: (Mo & White 1996, MW), (Sheth & Tormen 1999, ST), (Tinker et al. 2010, T), and (Pillepich et al. 2010, P).

where $\beta_w \equiv f/\tilde{b}_w(L)$. We have checked whether these expressions describe the ratios $r_\nu(L)$. To this end, the halo abundance $n(M)$ is taken to be described by the fitting formulae of Jenkins et al. (2001), which is suitable for simulations such as the L-BASICC. A crucial step is the choice of the halo-mass bias $b(M)$. In Fig. A.1 we show predictions for the ratio $r_3(L)$, obtained using some examples of prescriptions for this quantity: Mo & White (1996), Sheth & Tormen (1999), Tinker et al. (2010) and Pillepich et al. (2010)⁹. In order to witness the performance of these prescriptions, the bottom panels of Fig. A.1 show the luminosity bias obtained in a similar way as described by Eq. (7), using the estimates of the matter power spectrum of the L-BASICC II simulation. This figure shows that: *i*) as established by a number of studies, a scale dependent halo-mass bias is a fair modeling of the cluster power spectrum on large scales. *ii*) The Kaiser effect is a good description of the redshift space power spectra, at least within the range of masses and scales probed by our analysis (see e.g. Bianchi et al. 2012, for a broader discussion on this subject). *iii*) When assessing the capability of a model to retrieve, either cosmological or astrophysical information from one or two-point statistics, more accurate models of halo-mass bias are required in view of the small statistical errors expected from forthcoming surveys (see e.g. Cunha & Evrard 2010; Wu et al. 2010; Smith et al. 2012) with volumes comparable to that of the L-BASICC simulation. Finally, *iv*) the discrepancies between the different prescription of halo-mass bias are slightly diminished when we work with estimates of relative biases instead of absolute biases.

⁹ The differences between fitting formulae are likely caused by the different cosmological model used in the N-body simulations, the characteristics of the halo-identification algorithm and the way the biases are measured (i.e. either from the correlation function, the power spectrum or by means of count-in cells experiments).